1992ApJ...397..482S

THE ASTROPHYSICAL JOURNAL, 397:482–491, 1992 October 1
© 1992. The American Astronomical Society. All rights reserved. Printed in U.S.A.

FRACTIONATION OF CO IN THE DIFFUSE CLOUDS TOWARD ζ OPHIUCHI[1]

YARON SHEFFER,[2] S. R. FEDERMAN,[3] DAVID L. LAMBERT,[2] AND JASON A. CARDELLI[4]

Received 1992 January 10; accepted 1992 April 13

ABSTRACT

Ultraviolet spectra of interstellar CO lines from the diffuse clouds toward ζ Oph were obtained with the Goddard High Resolution Spectrometer on the *Hubble Space Telescope*. The ratios $a(\mathrm{CO}) \equiv N(^{12}\mathrm{C}^{16}\mathrm{O})/N(^{13}\mathrm{C}^{16}\mathrm{O}) = 150 \pm 27$ (1 σ) and $N(^{12}\mathrm{C}^{16}\mathrm{O})/N(^{12}\mathrm{C}^{17}\mathrm{O}) \simeq N(^{12}\mathrm{C}^{16}\mathrm{O})/N(^{12}\mathrm{C}^{18}\mathrm{O}) \gtrsim 800$ (3 σ) are derived from the $A\ ^1\Pi$–$X\ ^1\Sigma^+$ 5–0 and 6–0 bands at 1392 and 1367 Å, respectively, and published observations from *Copernicus* of weaker $^{12}\mathrm{C}^{16}\mathrm{O}$ A–X bands. Since a(CO) exceeds (by 3 σ) the intrinsic $^{12}\mathrm{C}/^{13}\mathrm{C}$ ratio of 70 as given by the CH^+ optical lines, CO is evidently fractionated on the smallest scale explored to date. The absence of $^{12}\mathrm{C}^{18}\mathrm{O}$ lines also indicates fractionation because the intrinsic ratio $^{16}\mathrm{O}/^{18}\mathrm{O}$ is likely to be close to the solar value of 500. The A–X bands and the $B\ ^1\Sigma^+$–$X\ ^1\Sigma^+$ 0–0 band, also observed with GHRS, are well matched with a total column density $N(\mathrm{CO}) = 2.2 \times 10^{15}$ cm^{-2} spread between two clouds separated by 1.2 km s^{-1} and at an excitation temperature $T_{ex} = 4.2$ K. The observed fractionation and excitation temperature suggest that the CO molecules reside in low-density gas [$n_H = n(\mathrm{H}) + 2n(\mathrm{H}_2) \simeq 100$–$200$ cm^{-3}].

Subject headings: ISM: abundances — ISM: molecules — stars: individual (Zeta Ophiuchi)

1. INTRODUCTION

The diffuse interstellar clouds along the line of sight to the bright O star ζ Ophiuchi are a rich source of interstellar absorption lines. Interstellar carbon monoxide through its ultraviolet electronic transitions $A\ ^1\Pi$–$X\ ^1\Sigma^+$, $B\ ^1\Sigma^+$–$X\ ^1\Sigma^+$, and $C\ ^1\Sigma^+$–$X\ ^1\Sigma^+$ has been the subject of several earlier studies that drew on spectra of ζ Oph acquired with the *Copernicus* or *IUE* satellites (e.g., Jenkins et al. 1973; Morton 1975; Smith, Krishna Swamy, & Stecher 1978; Wannier, Penzias, & Jenkins 1982, hereafter WPJ). In this paper we analyze spectra of the 5–0 and 6–0 bands of the A–X system and the 0–0 band of the B–X system obtained with the Goddard High Resolution Spectrometer (GHRS) on the *Hubble Space Telescope*. At a resolution of approximately 3 km s^{-1}, the rotational struture of the $^{12}\mathrm{C}^{16}\mathrm{O}$ and $^{13}\mathrm{C}^{16}\mathrm{O}$ bands is well resolved. By combining these new observations of the A–X bands with published measurements of weaker bands, we estimate the isotopic ratio $a(\mathrm{CO}) \equiv N(^{12}\mathrm{C}^{16}\mathrm{O})/N(^{13}\mathrm{C}^{16}\mathrm{O})$, where N is the total column density. Fractionation of CO is observed in absorption for the first time in a diffuse cloud; that is, $a(\mathrm{CO}) > a(\mathrm{CH}^+)$ where CH^+, which must be formed in warm gas, is considered to be unfractionated such that $a(\mathrm{CH}^+) \equiv N(^{12}\mathrm{CH}^+)/N(^{13}\mathrm{CH}^+) = N(^{12}\mathrm{C})/N(^{13}\mathrm{C})$. We also comment on the molecule's excitation temperature, provide a lower limit to the $^{16}\mathrm{O}/^{18}\mathrm{O}$ ratio, and remark on the absence of CO lines from the gas that provides broad CH^+ and CH lines which are commonly attributed to warm gas behind a shock front.

2. OBSERVATIONS AND REDUCTIONS

The ζ Oph CO data discussed here represent a subset of observations obtained as part of the GHRS in-flight science verification program. These observations were made using the GHRS high-dispersion echelle modes (Ech-A and Ech-B) in 1991 May (for specific instrument details see Duncan & Ebbets 1989; Cardelli, Ebbets, & Savage 1990) with the star placed in the 0.″25 × 0.″25 small science aperture (SSA) which, projected onto the 500 channel Digicon science diode array, is approximately the width of a single diode. The data were obtained with a substep sampling strategy corresponding to two samples per science diode width (3.15 km s^{-1} resolution) and a four position comb-addition for the purpose of reducing diode-to-diode variations. All observations were performed with the on-board Doppler compensator enabled, which compensates for the orbital motion of the spacecraft, and with the procedure FP-SPLIT = 4 (see Duncan & Ebbets 1989). This procedure, which divides each requested exposure into four subexposures each obtained at a slightly different grating position, is designed to reduce the effects of photocathode fixed pattern noise/granularity.

The general details about the reduction of GHRS echelle data applicable to the observations presented here are discussed in Cardelli et al. (1991). Briefly, the raw data from the 500 science diodes were converted to count rates, adjusted for pulse-counting dead-time losses, particle radiation, dark counts, and pixel-to-pixel variations. The individual spectrum substeps were merged to form a single spectrum of 1000 points in length. Wavelengths were assigned from standard calibration tables. The individual FP-SPLIT subexposures were aligned in diode space using observed spectral features as reference and combined. The final step in the reduction involved the subtraction of scattered light background. This background, which consists of the actual measured background in the inter-order above and below the spectral order, was converted to count rates, expanded to 1000 points, fitted with a low-order polynomial, and subtracted from the spectrum. An additional second-order background correction based on the results of Cardelli, Ebbets, & Savage (1990, 1992) was also applied. Mea-

[1] Based on observations obtained with the NASA/ESA *Hubble Space Telescope* through the Space Telescope Science Institute, which is operated by the Association of Universities for Research in Astronomy, Inc., under NASA contract NAS5-26555.

[2] Department of Astronomy, University of Texas, Austin, TX 78712. Electronic mail: yaron@astro.as.utexas.edu (Y. S.); dll@astro.as.utexas.edu (D. L. L.).

[3] Department of Physics and Astronomy, University of Toledo, Toledo, OH 43606. Electronic mail: sfederm@uoft02.utoledo.edu.

[4] Washburn Observatory, University of Wisconsin, Madison, WI 53706. Electronic mail: @vms.macc.wisc.edu:CARDELLI@MADRAF.decnet.

© American Astronomical Society • Provided by the NASA Astrophysics Data System

1992ApJ...397..482S

surements of the continuum rms in the three final net spectra containing the B–X 0–0, A–X 5–0, and 6–0 CO lines corresponded to signal-to-noise values of about 24, 65, and 75, respectively. A spectrum of the A–X 5–0 band was also obtained through the large science aperture (LSA). The spectrum is of lower resolution (Fig. 1), but of appreciably higher S/N ratio ($\simeq 170$) than the comparable SSA spectrum. The LSA spectrum provides the more accurate estimate of equivalent widths (W_λ) of the bands and especially of the weak $^{13}C^{16}O$ band and an upper limit to the W_λ of the undetected $^{12}C^{17}O$ and $^{12}C^{18}O$ bands. The principal $^{12}C^{16}O$ lines (Fig. 1) are highly saturated. Although the rotational structure is resolved, the profiles of the individual lines are essentially that of the spectrometer, and the much narrower intrinsic profile is essentially irrecoverable. In Table 1 we give the measured W_λ (and 1 σ errors) for the individual lines and for the band. For the $^{12}C^{16}O$ bands, the total W_λ is in good agreement with WPJ's estimates from the lower resolution *Copernicus* spectra in which the R and Q branches were only partially resolved. Less accurate W_λ were also given by WPJ from *IUE* spectra. The GHRS W_λ for the B–X 0–0 band is somewhat smaller than WPJ's measurement from Copernicus spectra. The W_λ of the $^{13}C^{16}O$ bands are discussed below.

In the absence of wavelength calibration observations, internal errors in the assigned wavelengths as large as ± 1 diode (± 3 km s^{-1}) for a single observation are expected (see Cardelli et al. 1991). From an analysis of the complete set of lines observed in the ζ Oph data, we found a dispersion of ± 2.2 km s^{-1} about the average line velocity. In addition, external errors associated with the correction for spacecraft motion can also occur, as was found from an analysis of telluric O I lines in GHRS echelle data of ζ Per (Cardelli, Savage, & Ebbets 1991). We applied their bootstrap technique in order to compensate for wavelength errors. In short, lines of a particular species arising in different observations are aligned in velocity space. As a consequence, lines from other species present in these observations are thus "corrected" to the same relative velocity scale. Other observations can subsequently be "corrected" to this reference system by using lines common to these other species. In the case of the ζ Oph data, there was insufficient correspondence of lines from similar species between the different observations, and so we expanded the technique to include the alignment of lines from species with similar depletion characteristics. In the end, all the data were referenced to the Mn II 1199 Å line which was chosen as a reference because it is present in the same observation with telluric N I lines (the 1200 Å triplet). The final step involved correcting the measured velocity of the telluric lines to what is expected for the velocity of Earth's atmosphere relative to the spacecraft at the time of the observation (see Savage, Cardelli, & Sofia 1992 for further details). Based on a comparison of our final velocities to those from high-dispersion ground-based absorption-line data (Hobbs 1973), we estimate the final velocities to have an error of about ± 1 km s^{-1} relative to the heliocentric reference frame. Following the bootstrap wavelength calibration, the heliocentric velocity is -13 ± 1 km s^{-1}, indicating an origin, as expected, in the main cloud complex toward ζ Oph which is also responsible for numerous other atomic and molecular lines. Note that all isotopic species belonging to the same band are observed simultaneously in a single spectrum.

Rest wavelengths of the resolved 5–0 and 6–0 transitions were computed from the molecular constants of Mantz et al.

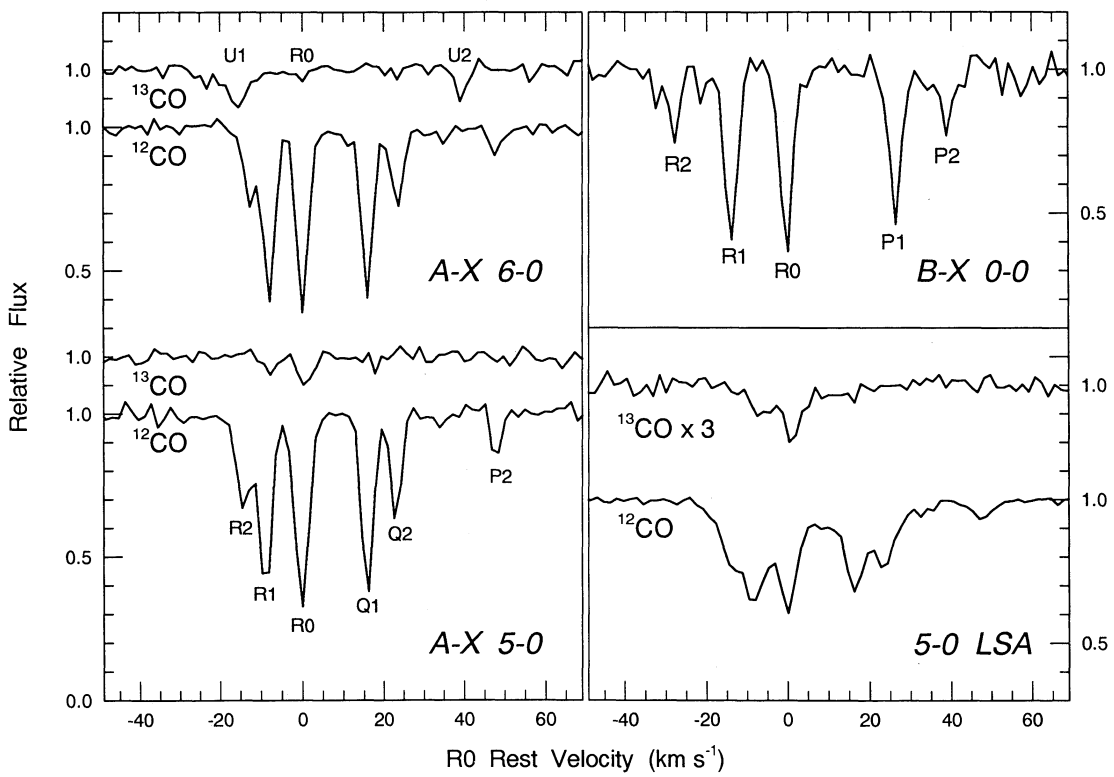

FIG. 1.—GHRS spectra of the CO $A\ ^1\Pi$–$X\ ^1\Sigma^+$ 5–0 and 6–0 and $B\ ^1\Pi^+$–$^1X\ ^1\Sigma^+$ 0–0 bands. The montage in the left-hand panel shows the $^{12}C^{16}O$ and $^{13}C^{16}O$ A–X bands as observed through the SSA. These spectra are aligned so that the $R(0)$ lines define the velocity scale; the separations of rotational lines of the 5–0 and 6–0 bands are similar. Note the two unidentified lines in the interval showing the 6–0 $^{13}C^{16}O$ band (*see text*). The lower right-hand panel shows the LSA spectra of the A–X 5–0 bands with an expanded flux scale of ^{13}CO relative to that of ^{12}CO. The upper right-hand panel shows the SSA spectrum of the B–X 0–0 ^{12}CO band.

© American Astronomical Society • Provided by the NASA Astrophysics Data System

1992ApJ...397..482S

TABLE 1

EQUIVALENT WIDTHS OF A–X AND B–X LINES

	W_λ(mÅ)				
	^{12}CO A–X		^{13}CO A–X		^{12}CO B–X
LINE/BAND	5–0	6–0	5–0	6–0	0–0
$R(2)$[a]	7.5	4.7	0.2	...	3.0
$R(1)$	10.5	9.7	0.7	...	8.7
$R(0)$	13.2	10.6	1.9	0.8	9.2
$Q(1)$[b]	11.1	9.6	0.6	...	...
$Q(2)$[b]	5.7	4.8	...	...	...
$Q(3)$[b]	0.6	0.6	...	...	...
$P(1)$[b]	...	...	...	...	7.1
$P(2)$	2.2	1.6	...	...	3.0
$P(3)$	0.3	0.6	...	...	...
GHRS	48.8 ± 1.8[c]	44.2 ± 1.8	3.6 ± 0.3[c]	1.4 ± 0.4[d]	32.5 ± 2.5
WPJ-*IUE*	46 ± 10	45 ± 8	9.7 ± 4.2	...	...
WPJ-C	51.5 ± 5.6	44.0 ± 3.1	...	5.9 ± 0.7	38 ± 1.5

[a] For the A–X bands, the W_λ includes a small contribution from the unresolved R(3) line.
[b] The A–X bands do not have a $P(1)$ line, and the Q branch is forbidden for the B–X transition.
[c] For the 5–0 band, the W_λ values are from the LSA spectrum.
[d] W_λ from $J > 0$ has been estimated.

(1975) and Tilford & Simmons (1972). The appropriate reduced mass ratios were applied to these constants in order to derive the isotope shifts relative to Kurucz's (1976) wavenumbers of $^{12}C^{16}O$. In the 5–0 spectrum the observed $^{12}C^{16}O$ and $^{13}C^{16}O$ lines match the predictions to within 1 km s^{-1}, or less than 1 pixel (see Fig. 1). A subpixel discrepancy in the ^{13}CO wavelengths relative to the ^{12}CO lines was noted. At our request, C. M. Brown (1991, private communication) remeasured laboratory spectra of a $C^{18}O$–enriched source, which revealed a 1 km s^{-1} shift relative to calculated values for the $^{12}C^{18}O$ lines. This shift completely accounts for the subpixel velocity shift between ^{12}CO and ^{13}CO, on the plausible assumption that the systematic errors of the predicted isotopic shifts of ^{13}CO and $^{12}C^{18}O$ (relative to $^{12}C^{16}O$) are quite similar. For the 5–0 bands we employ the LSA W_λ values, which are confined by the SSA spectrum.

In the region of the $^{13}C^{16}O$ and $^{12}C^{18}O$ 6–0 bands, there are two obvious interstellar lines (Fig. 1). One line was on superficial examination identified as the $R(0)$ $^{13}C^{16}O$ line. Closer inspection shows that the predicted wavelength is 15 km s^{-1} to the red of the interstellar line. We consider the 15 km s^{-1} shift to be much larger than can be attributed to uncertainties in the GHRS's wavelength calibration and in the predicted wavelengths. Therefore, we suppose that the line is in fact an unidentified interstellar line. The line has a rest/laboratory wavelength $\lambda = 1370.61$ Å and $W_\lambda = 4.0$ mÅ. The other interstellar line nearly coincident with the $R(0)$ $^{12}C^{18}O$ line is quite obviously too strong to be due to this rare form of the CO molecule. This second unidentified line at $\lambda = 1370.87$ Å with $W_\lambda = 1.6$ mÅ was noted also by Cardelli et al. (1991). When the predicted wavelengths are adopted, only $R(0)$ of the 6–0 $^{13}C^{16}O$ band is marginally identified above the noise; the corresponding total W_λ in Table 1 is an estimated upper limit for the band. The 5–0 $^{12}C^{17}O$ and $^{12}C^{18}O$ bands are not detectable in the LSA spectrum. We estimate $W_\lambda \lesssim 0.4$ mÅ as a 3 σ upper limit for the $R(0)$ line in these bands. The lower S/N but higher resolution SSA spectra of the 5–0 and 6–0 bands set a less stringent upper limit.

The wavelengths for the B–X 0–0 band were taken from WPJ. The isotopic wavelength shifts, $\lambda(^{12}CO)$–$\lambda(^{13}CO)$, are less than about 10 mÅ (Eidelsberg et al. 1987) for this band.

3. THE ISOTOPIC RATIOS $^{12}C/^{13}C$ AND $^{16}O/^{18}O$

Since the 5–0 and 6–0 bands are highly saturated, an accurate estimate of the column density $N(^{12}C^{16}O)$ is unobtainable from these bands. Therefore, we obtain the ratio a(CO) by using the weakest ^{12}CO A–X bands measured by WPJ and our new more accurate measurements of the ^{13}CO bands. All of the observed ^{12}CO A–X bands were used to define a curve of growth, the relation between the W_λ and the f-values of the bands. We assumed that the curves of growth for ^{12}CO and ^{13}CO bands are identical. Then, the ratio a(CO) follows by fitting the curve of growth to the ^{13}CO points. This is precisely how WPJ obtained their estimate of $a(\mathrm{CO}) = 55 \pm 11$.

Construction of the curve of growth requires a set of f-values for the A–X system bands. Radiative lifetimes of vibrational levels of the $A\ ^1\Pi$ state have been measured by many investigators. A thorough discussion of their own and previously published measurements is given by Field et al. (1983) who corrected their measurements for levels $v' = 0$–7 for the effects of the perturbations by various triplet states. The "deperturbed" lifetimes were used to derive the electronic transition moment $R_e(r)$ which was assumed to be linear in the internuclear separation r. Then, it is a simple matter to derive f-values for individual bands from the standard relation

$$f_{v'v''} = 3.04 \times 10^{-6} g q_{v'v''} \sigma_{v'v''} |R_e(\bar{r}_{v'v''})|^2 ,$$

where R_e is expressed in atomic units, $q_{v'v''}$ is the Franck-Condon factor, $\bar{r}_{v'v''}$ is the r-centroid, and $\sigma_{v'v''}$ (in cm^{-1}) is the frequency of the band orgin. The factor $g = (2 - \delta_{0,\Lambda'+\Lambda''})/(2 - \delta_{0,\Lambda'}) = 2$ for the A–X system. We take $q_{v'v''}$ and $\bar{r}_{v'v''}$ from Kurucz (1976) who tabulates predictions for RKR potentials for the A and X states. This procedure gives the $f_{v'v''}$ values for all required bands provided that the low rotational lines of the $(v', 0)$ bands of interest are not perturbed and the $\bar{r}_{v'v''}$ lies within the range sampled by τ_v measurements for $v' = 0$–7.

WPJ's measurements of the weak 12–0 and 11–0 $^{12}C^{16}O$ A–X bands are the most relevant to the determination of a(CO) because they span the W_λ range of the observed ^{13}CO bands. For the 12–0 and 11–0 bands, the $\bar{r}_{v'v''}$ lies slightly outside the range sampled by Field et al.'s $\tau_{v'}$ measurements. Extrapolation of their linear $R_e(r)$ is unlikely to be a serious

© American Astronomical Society • Provided by the NASA Astrophysics Data System

1992ApJ...397..482S

source of error because the extrapolation is slight. Certainly, the inferred $f_{v'v''}$-values agree to within 10% with values derived by Lassettre & Skerbele (1971) from their electron-scattering experiments; WPJ tabulate $f_{v'v''}$-values from Lassettre & Skerbele. In addition, the $f_{v'v''}$-values, as given by Field et al.'s (1983) $R_e(r)$, are in fair agreement with results of ab initio calculations by Kirby & Cooper (1989): the calculated ratio $f_{10,0}/f_{5,0}$ is within 10% of the value from Table 2. Unfortunately, Kirby & Cooper do not tabulate the $f_{11,0}$ and $f_{12,0}$ values. The slope of the ab initio $R_e(r)$ differs somewhat from that given by Field et al., and as a consequence, the variations of $f_{v'v''}$ with v' are slightly different: for example, the ratio $f_{10,0}/f_{5,0}$ is about 20% larger from the ab initio calculation than from Field et al.'s $R_e(r)$. Finally, our estimate is in accord with the recent work of the Meudon group on f-values for $v' \leq 12$ (F. Rostas 1991, private communication; see Eidelsberg et al. 1992); for $f_{12,0}$ and the ratio $f_{12,0}/f_{5,0}$, our values are within 20% of theirs. Our assumption that a $f_{v'v''}$-value is the same for ^{12}CO and ^{13}CO is valid unless a band from one or both species is perturbed at the lowest J-values ($J = 0$, 1, and 2).

Our W_λ are adopted for the 5–0 and 6–0 bands. For all other bands we take the measurements reported by WPJ and give preference to those measurements made from *Copernicus* spectra. Adopted W_λ are listed in Table 2, where the higher signal-to-noise LSA results are used for the 5–0 bands. In Figure 2 we show log W_λ versus log $\lambda^2 f_{v'v''}$ for the ^{12}CO and ^{13}CO bands. The line representing the ^{12}CO curve of growth is a band synthesis prediction for the two-cloud model discussed later. The line fits essentially all but one of the points within the measurement errors. The exception is the 1–0 band. We suppose that its W_λ has been overestimated; perhaps the band is blended with another interstellar line.

Translation of the ^{12}CO curve of growth to fit the ^{13}CO points provides the ratio a(CO). The derived ratio is not dependent on the use of the theoretical curve of growth; an empirical curve of growth gives an identical result. Three of the four ^{13}CO bands yield a consistent ratio. We base our estimate of $a(\mathrm{CO}) = 150 \pm 27$ (1 σ) on our measurement of the 5–0 ^{13}CO band where the uncertainty is the quadratures sum of the W_λ errors for the 5–0 band and the 12–0 ^{12}CO bands. The 4–0 ^{13}CO band as measured by WPJ confirms the a(CO) estimate. Our upper limit to W_λ for the 6–0 ^{13}CO band is 1.8 mÅ, a little below the expected value for $a(\mathrm{CO}) = 150$. The larger than expected W_λ of the 2–0 ^{13}CO band remains unexplained: $a(\mathrm{CO}) \simeq 30$ is needed to fit this band. We suppose that either W_λ from *IUE* spectra has been overestimated or the band is blended. The upper 3 σ limit to the W_λ of the 5–0 ^{12}C^{17}O and ^{12}C^{18}O bands corresponds to a higher isotopic ratio, that is, $N(^{12}\mathrm{C}^{16}\mathrm{O})/N(^{12}\mathrm{C}^{17}\mathrm{O}) \simeq N(^{12}\mathrm{C}^{16}\mathrm{O})/N(^{12}\mathrm{C}^{18}\mathrm{O}) \gtrsim 800$.

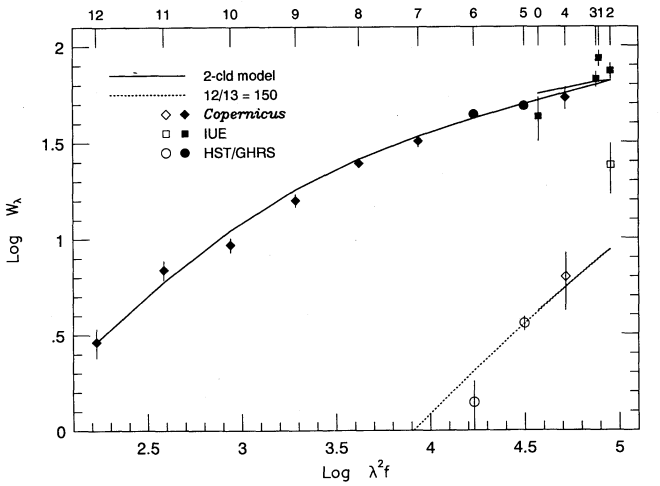

FIG. 2.—The ^{12}CO and ^{13}CO curves of growth (log W_λ vs. log $f_{v'v''}\lambda^2$) for the A–X bands. Open symbols denote the ^{13}CO bands. The predicted curve of growth is provided by the two-cloud model described in the text. Bands v'–0 from $v' = 0$–12 are represented by the solid line and are identified by the numbers at the top of the figure.

TABLE 2

THE CO A–X BANDS

Transition	λ(Å)	log $f_{v'v''}$	W_λ(mÅ)	Reference for W_λ
		^{12}C^{16}O		
12–0.....	1246	−3.97	2.9 ± 0.4	WPJ-C
11–0.....	1263	−3.62	6.9 ± 0.8	WPJ-C
10–0.....	1281	−3.28	9.3 ± 0.8	WPJ-C
9–0.....	1301	−2.94	15.7 ± 1.2	WPJ-C
8–0.....	1322	−2.62	24.6 ± 1.3	WPJ-C
7–0.....	1344	−2.32	32.0 ± 2.2	WPJ-C
6–0.....	1367	−2.04	44.2 ± 1.8	This paper
5–0.....	1392	−1.79	48.8 ± 1.2	This paper
4–0.....	1419	−1.59	53.9 ± 7.1	WPJ-C
3–0.....	1447	−1.44	66 ± 6	WPJ-*IUE*
2–0.....	1477	−1.39	74 ± 7	WPJ-*IUE*
1–0.....	1509	−1.46	86 ± 8	WPJ-*IUE*
0–0.....	1544	−1.81	43 ± 11	WPJ-*IUE*
		^{13}C^{16}O		
6–0.....	1371	−2.04	1.4 ± 0.4	This paper
5–0.....	1395	−1.79	3.6 ± 0.3	This paper
4–0.....	1421	−1.59	6.3 ± 2.1	WPJ-C
2–0.....	1478	−1.39	24 ± 7	WPJ-*IUE*

Since the $A\ ^1\Pi$ state is well known to be subject to many perturbations from overlying triplet states, the adopted f-values will be inappropriate when lines from perturbed levels are used. As the triplet states have much longer radiative lifetimes than the $A\ ^1\Pi$ state, the effect of a perturbation is to increase the lifetime of the perturbed $A\ ^1\Pi$ level and, hence, the f-value for lines from such a level is less than that derived from the adopted $f_{v'v''}$-value (Field et al. 1983; Le Floch, Rostas, & Rostas 1990). This might suggest that the aberrant ^{13}CO bands are the 4–0, 5–0, and 6–0, not the 2–0. We dismiss this possibility. First, perturbations necessarily shift the energy levels, and no such shifts for the 5–0 band are suggested by the interstellar ^{13}CO lines. Second, the f-value reductions are generally confined to lines involving a single common level in the $A\ ^1\Pi$ state, and, hence, a perturbed and is likely to give an anomalous excitation temperature (see Le Floch et al.'s 1990, Fig. 4). Third, the f-value reductions are often small for A–X lines. Fourth, the lack of scatter of the ^{12}CO points about the smooth curve of growth suggests that perturbations are a rare occurrence.

Our isotopic ratio of a(CO) = 150 is a factor of 3 higher than WPJ's estimate of 55. The principal reason for this large difference is that WPJ ignored the higher value of a(CO) implied by the 4–0 ^{13}CO band and based their result on the 5–0 and 6–0 ^{13}CO bands for which we obtain smaller W_λ. WPJ's W_λ of 5.9 ± 0.7 mÅ for the 6–0 band is larger than our upper limit, but this difference arises *because we believe the prominent line near this band is not due to CO*. Our measured W_λ, including this line, is $W_\lambda \simeq 5 \pm 1$ mÅ, a value consistent with WPJ's result. The higher resolution spectra obtained with the GHRS enable us to separate the ^{13}CO lines from the stronger

© American Astronomical Society • Provided by the NASA Astrophysics Data System

1992ApJ...397..482S

unidentified line. WPJ's value of $W_\lambda = 9.7 \pm 4.2$ mÅ for the 5–0 band is nearly 3 times larger than our more accurate LSA result, which is confirmed by our independent SSA exposure. With WPJ's W_λ, the 5–0 and 6–0 bands gave consistent estimates of a(CO). With our W_λ the two bands also give consistent estimates of a(CO). The f-values (Lassettre & Skerbele 1971) adopted by WPJ are similar to those used by us. In particular, the ratios relevant to the estimation of a(CO) such as $f_{12,0}/f_{5,0}$ are identical to better than 5%. Hence, the adopted f-values are not responsible for the different a(CO) values.

In § 5 we compare our determination of a(CO) with the isotopic ratio $^{12}C/^{13}C(=70)$ as given by observations of the CH^+ 4232 Å line. Here we comment briefly on the use of the CO rotational lines to obtain a(CO) for the ζ Oph clouds. Crutcher & Watson (1981) failed to detect the ^{13}CO 1–0 line and gave $a(CO) > 50$ as a "very conservative" upper limit. Langer, Glassgold, & Wilson (1987, hereafter LGW) report a detection of the ^{13}CO line and give a(CO) over the whole velocity interval as "about 80 with a 3 σ range from 50 to 300". For the stronger component at -0.72 km s^{-1}, they obtained the value for a(CO) of 141^{+77}_{-38} (1 σ errors). The lower integrated value is a consequence of the smaller ratio for the weaker component(s), which are resolved in the radio measurements. Since we do not resolve the two main components, it is possible that an even higher fractionation [$a(CO) > 150$] is present in the strongest component. However, since radio observations use beams 1′–2′ in size, they tend to be contaminated by contributions from cloud components over a relatively large sky area, both in front and behind ζ Oph (see LGW). Our UV data are highly localized on the line of sight in front of the stellar disk, the area of the optical "beam" being roughly 10 orders of magnitude smaller than the radio beams. A similar ratio also holds for the corresponding volumes being probed. Our fractionation result, therefore, is of the highest relevance to microscopic conditions in the gas, also to be discussed in § 5.

4. THE CO COLUMN DENSITY AND EXCITATION TEMPERATURE

4.1. *Diffuse Clouds*

The two ^{12}CO bands observed with the GHRS are highly saturated, and, hence, the W_λ of such a band is sensitive to the presence of multiple clouds, the level of turbulence within each cloud, and the molecule's excitation temperature. Also, these bands may permit detections of lines from higher rotational levels or weak broad components from the warm gas providing the CH^+ 4232 Å line. For such reasons, we have constructed theoretical band profiles and curves of growth using other observations.

Observations of the CO 1–0 and 2–1 lines at millimeter wavelengths—with resolution (R) of up to 4,600,000—have provided clear evidence for two (or more) diffuse clouds along the line of sight to ζ Oph—see Crutcher & Federman (1987), LGW, and Le Bourlot, Gerin, & Perault (1989). $R = 600{,}000$ optical spectra of the CN 3874 Å and CH 4300 Å lines also showed the presence of two clouds (Lambert, Sheffer, & Crane 1990). By contrast, the CH^+ 4232 Å line, which cannot be formed in the cool clouds responsible for the bulk of the CN and CO, is broader (FWHM $\simeq 3.5$ km s^{-1}) and apparently single. This gas, which is expected to be much warmer than the bulk of the diffuse clouds, also contributes to the CH line where it provides an even broader (FWHM $= 5.2$ km s^{-2}) line. A second even broader component makes a weak contribution to the CH^+ line (Crane, Hegyi, & Lambert 1991). We discuss in § 4.2 a possible contribution of the broad-line region to the CO lines.

Our calculations show that the W_λ of the CO A–X bands are well explained when the CO is supposed to exist in two clouds whose velocity separation and turbulences are compatible with the observed values from the millimeter and optical lines. In Figure 3 we show the observed and predicted run of W_λ versus v' for the A–X bands from $v' = 0$–12. The predictions are a good fit to the observations except for the 1–0 $^{12}C^{16}O$ band. We suspect that the W_λ uncertainties have been underestimated or the 1–0 band is blended. (The discrepant 2–0 $^{13}C^{16}O$ band was discussed earlier.) The illustrated predictions correspond to two clouds having a total column density $N(^{12}CO) = 2.2(\pm 0.4) \times 10^{15}$ cm^{-2} at an excitation temperature $T_{ex} = 4.2(\pm 0.3)$ K. The total column density is constrained by the weak bands, especially by the 12–0 band, and is independent of the adopted cloud models. The predicted W_λ of the strong bands are sensitive to the adopted models. For our calculations, the relative contributions of the clouds are taken to be $N_1/N_2 = 3$ with a velocity separation (1.18 km s^{-1}) set at the value observed for CO by Le Bourlot et al. (1989) and for CN by Lambert et al. (1990). The widths (FWHM in km s^{-1}) of the absorption coefficients of the two clouds correspond to $\Delta v_1 = 0.58$ (the average of all millimeter observations) and $\Delta v_2 = 0.50$ (adopted representative value). Turbulence must be the dominant contributor to Δv_1 and Δv_2. The thermal width for $T = 50$ K, the mean kinetic temperature of the CO molecules (see below), is 0.29 km s^{-1}. Le Bourlot et al. found $\Delta v_1 = 0.60 \pm 0.01$ and $\Delta v_2 = 0.86 \pm 0.03$. Lambert et al. obtained $\Delta v_1 = 0.98 \pm 0.06$ and $\Delta v_2 = 0.64 \pm 0.13$ from the CN 3874 Å line. Calculations that adopt either of these latter sets of values for (N_1, Δv_1) and (N_2, Δv_2) or the four-cloud model offered by LGW reproduce the observed run of W_λ with v' provided that T_{ex} is reduced to about 3.2 K, but examination of the predicted and observed spectra for the 5–0 and 6–0 ^{12}CO bands show that, while these alternative models reproduce the bands' W_λ, such a T_{ex} is too low to account for the relative strengths of the rotational lines.

The much weaker $^{13}C^{16}O$ bands do offer a chance to estimate T_{ex} independently of the adopted line widths. In Figure 4 we show the observed and predicted spectra for the 5–0 $^{12}C^{16}O$ and $^{13}C^{16}O$ bands for the two-cloud model adopted

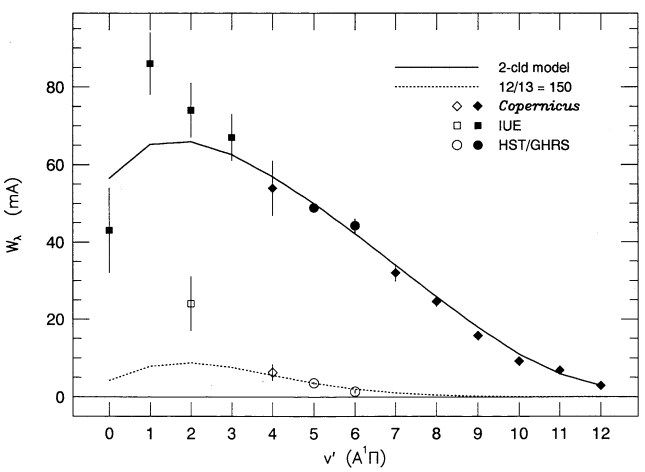

FIG. 3.—The variation of the equivalent widths (W_λ) of the A–X v'–0 bands with the vibrational quantum number (v') of the upper state. The prediction (*solid line*) is for the two-cloud model described in the text. The key to the observed W_λ is given in the figure.

© American Astronomical Society • Provided by the NASA Astrophysics Data System

1992ApJ...397..482S

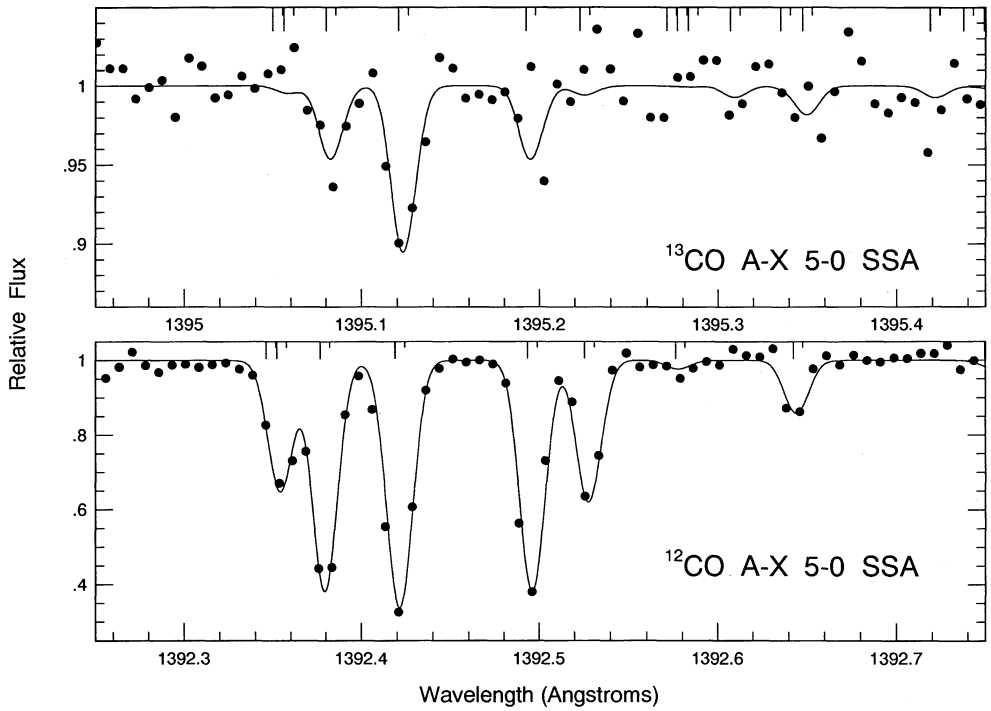

FIG. 4.—Observed and predicted spectra of the A–X 5–0 $^{12}C^{16}O$ and $^{13}C^{16}O$ bands. Note the expanded flux scale of ^{13}CO relative to that of ^{12}CO. Locations of the CO lines are marked at the top of the figures where the vertical tick is proportional to the column density. Each CO line is represented by two components (*see text*). The $^{12}C^{18}O$ band, here modeled by a column density $N(^{12}C^{18}O) = N(^{12}C^{16}O)/1000$, lies roughly 0.23 Å to the red of the ^{13}CO lines.

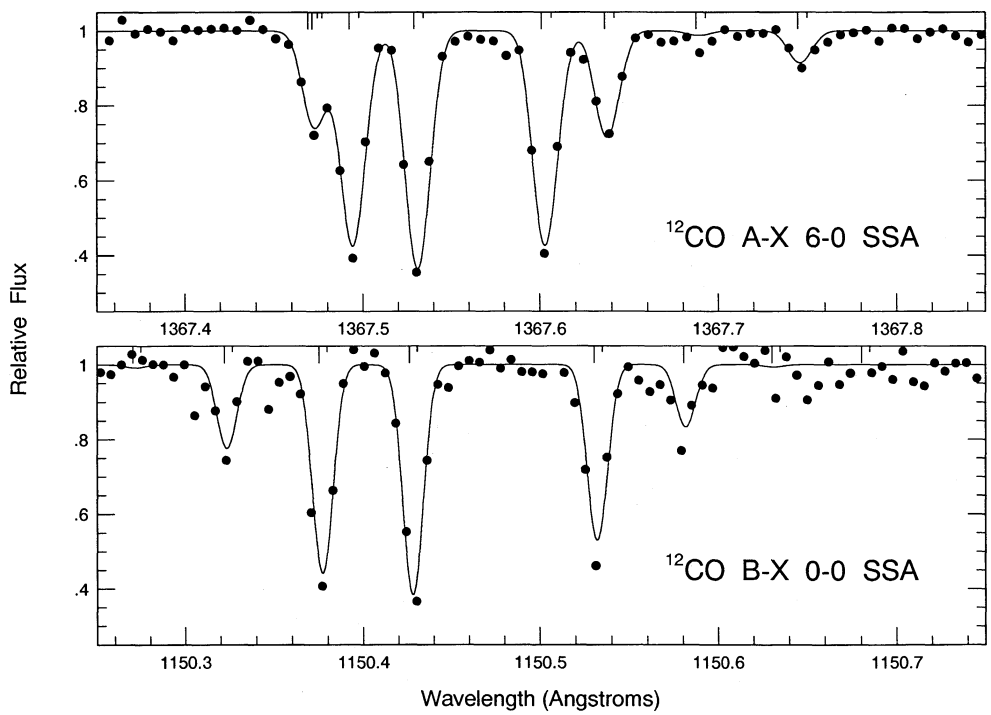

FIG. 5.—Observed and predicted spectra of the A–X 6–0 (*top*) and (*bottom*) B–X 0–0 (*bottom*) band

© American Astronomical Society • Provided by the NASA Astrophysics Data System

1992ApJ...397..482S

for Figure 3. The chosen $T_{ex} = 4.2$ K is an adequate fit to the rotational structure of both bands. The SSA spectrum of the 5–0 $^{13}C^{16}O$ band admits a temperature as high as $T_{ex} \sim 6$ K, but the LSA spectrum despite its lower resolution confirms that $T_{ex} \simeq 4$ K. We have assumed that the levels $J = 0$, 1, 2, and 3 may be described by a single value of T_{ex}. Such a single value provides a satisfactory fit to the spectra. On the assumption that the excitation temperatures for the ^{12}CO and ^{13}CO levels are identical, the fit to the 5–0 ^{13}CO band confirms the T_{ex} estimate made via Figure 3 from the strong ^{12}CO bands. The excitation temperatures of the two species are expected to be similar, but not neccessarily identical (see below). The fit to the 6–0 ^{12}CO band is shown in the top panel of Figure 5.

The adopted two-cloud model also accounts reasonably well for the observed B–X 0–0 ^{12}CO band. The f-value $f_{0,0} = 0.0058 \pm 0.0006$ is adopted based on a compilation (Krishmakumar & Srivastava 1986) of f-value or radiative lifetime measurements for the $B\ ^1\Sigma^+$ state. Observed and predicted spectra are compared in the bottom panel of Figure 5. The observed W_λ for the band is 32.5 ± 2.5 mÅ (Table 1) and the predicted $W_\lambda = 28.8 \pm 0.9$ mÅ. For the C–X system, Krishnakumar & Srivastava's compilation suggests $f_{0,0} = 0.10 \pm 0.02$, but the individual entries range widely ($f_{0,0} = 0.003$–0.16) so that selection of a "best" value is somewhat uncertain. Ab initio calculations (Kirby & Cooper 1989) predict $f_{0,0} = 0.12$. (These calculations also predict $f_{0,0} = 0.0021$ for the B–X 0–0 band.) WPJ list the W_λ of the C–X 0–0 band as 82 mÅ, but this estimate must include the C I line at 1088 Å (Federman 1986; see Smith et al. 1978 for a comparison of observed and predicted profiles). Our prediction is $W_\lambda = 48.6 \pm 1.5$ mÅ for $f_{0,0} = 0.10 \pm 0.02$.

4.2. *The Warm Gas*

As is well known (Federman 1982), insterstellar CH^+ molecules cannot be formed in the observed abundance in cool diffuse clouds. Warm gas with a temperature of a couple of thousand degrees is needed to ensure adequate production of CH^+ through the endothermic reaction: $C^+ + H_2 \rightarrow CH^+ + H$. Following a suggestion by Elitzur & Watson (1980), the necessary warm gas has generally been identified with gas behind a shock front. However, it is unclear whether the column density required to provide the strong CH^+ line seen in ζ Oph's spectrum can be manufactured behind a shock (Lambert et al. 1990). Here we shall simply refer to the CH^+ line as arising in "warm" gas. This warm gas as revealed by the CH^+ and the broad component of the CH lines is both warm and turbulent. High-resolution spectra show the CH^+ line to have $\Delta v = 3.5$ km s^{-1} and the associated component of the CH line to have $\Delta v = 5.2$ km s^{-1} (Lambert et al. 1990).

To assess the limits on the column density of CO from the warm gas, we compared the observed A–X 5–0 and 6–0 ^{12}CO profiles with predictions for different amounts of "warm" CO. The predicted spectra were convolved with the estimated instrumental profile. If the widths of lines from the warm gas are dominated by turbulence rather than the thermal velocities, we suppose $\Delta v = 5.2$ km s^{-1} may be appropriate for the CO component. Then, the limit on the column density is $N(CO)_w \lesssim 4 \times 10^{13}$ cm^{-2}, or 2% of the total column density. If thermal velocities are dominant, the CO component will be narrower ($\Delta v = 2.4$ km s^{-1}) than its CH and CH^+ counterparts, and the limit on the column density rises to $N(CO)_w \lesssim 8 \times 10^{13}$ cm^{-2}. Inspection of the spectra shows that the warm gas must also have a low excitation temperature as there is no indication of absorption from levels with $J > 3$.

5. CHEMICAL CONSIDERATIONS

5.1. *CO from Warm Gas*

Theoretical predictions are consistent with our inability to detect CO arising from the warm (shocked?) gas needed to produce the observed amount of CH^+. Mitchell & Watt (1985) discussed three routes to CO:

$$CH + O \rightarrow CO + H\,, \tag{1}$$

$$C^+ + OH \rightarrow CO^+ + H\,, \tag{2}$$

$$CH^+ + O \rightarrow CO^+ + H\,. \tag{3}$$

In the latter two cases CO is formed when HCO^+ dissociatively recombines with an electron; HCO^+ is produced through a hydrogen abstraction reaction involving CO^+. The column density of CO produced in this way is given by

$$N(CO)_w = \frac{x(O)[N(CH)_w k_1 + N(CH^+)_w k_3] + N(OH)_w x(C^+) k_2}{\Gamma(CO)/n_H}\,. \tag{4}$$

The quantities $N(S)$ and $x(S)$ are the column density and abundance, respectively, of species S; k_i are rate coefficients; n_H is the density of hydrogen nuclei; and $\Gamma(CO)$ is the photodissociation rate of CO. For the rate coefficients, we used $k_1 = 9.5 \times 10^{-11}\,(T/300)^{0.5}$ (Messing et al. 1981), $k_2 = 2.0 \times 10^{-9}$ (Glassgold & Langer 1976), and $k_3 = 3.5 \times 10^{-10}$ (Anicich & Huntress 1986), all in units of cm^3 s^{-1}. The photodissociation rate was set to 1×10^{-10} s^{-1}, allowing for some grain attenuation, but no self-shielding. Self-shielding does not play a role when $N(CO) \sim 10^{13}$ cm^{-2}. The respective abundances for O and C^+ were 3.5×10^{-4} and 2.5×10^{-4}. We estimated a density of 100 cm^{-3} and a temperature of 1000 K for the warm gas. For the column densities pertaining to the warm gas, the prediction of Draine (1986) for OH and the observations of Lambert et al. (1990) for CH and CH^+ were used. The resulting value for $N(CO)_w$ is 5.4×10^{12} cm^{-2}, which is well below our detection limit of $N(CO)_w \leq 4$–8×10^{13} cm^{-2}. Thus, the absence of a broad component to the CO profiles is consistent with the carbon chemistry of the warm (shocked) gas.

5.2. *The $^{12}C/^{13}C$ Ratio*

Our discussion assumes that the $^{12}C/^{13}C$ ratio provided by the CH^+ 4232 Å line is the true (unfractionated) ratio $N(^{12}C)/N(^{13}C)$ of the clouds toward ζ Oph. This assumption is widely made on the grounds that the CH^+ molecules must reside in warm gas so that isotopic exchange reactions can have a negligible effect. For the $^{12}C/^{13}C$ ratio from CH^+, we adopt $^{12}C/^{13}C = 70 \pm 3$ as given by recent analyses of high S/N spectra of the CH^+ lines (Crane et al. 1991; Stahl & Wilson 1992; Stahl et al. 1989). If the lower ratio, $^{12}C/^{13}C = 45$ suggested by Hawkins & Jura (1987) and Hawkins et al. (1989) is preferred, the fractionation exhibited by CO is even more severe than we suppose. With our measured ratio [$a(CO) = 150 \pm 27$] and the assumed intrinsic ratio [$^{12}C/^{13}C = a(CH^+) = 70 \pm 3$], CO is clearly seen to be fractionated. We assume that the two clouds are fractionated to an identical degree. Our lower 3 σ limit to $N(^{12}C^{16}O)/N(^{12}C^{18}O)$ of 800 also suggests fractionation because the intrinsic ratio $^{16}O/^{18}O$ is likely to be close to the solar system's ratio of 500. The rare species $^{12}C^{17}O$ is presumably fractionated too, but even the intrinsic ratio which is probably close to the solar ratio of 2600 is far in excess of our observational 3 σ lower limit.

© American Astronomical Society • Provided by the NASA Astrophysics Data System

1992ApJ...397..482S

The observed ratio of $^{12}CO/^{13}CO$ is affected by a combination of isotopic charge exchange (Watson, Anicich, & Huntress 1976) and selective isotopic photodissociation (Bally & Langer 1982). Isotopic exchange enhances the amount of ^{13}CO relative to ^{12}CO because of the lower zero-point energy of ^{13}CO. Since CO is photodissociated by line radiation, ^{13}CO is destroyed preferentially because the more abundant ^{12}CO is self-shielded to a greater extent. The result that $a(CO)$ exceeds $a(CH^+)$ suggests that selective isotopic photodissociation is the dominant effect. To explore this suggestion, we suppose the CO density to be set by three processes: formation through collisions between $C^+ + OH$, photodissociation of CO, and isotopic exchange between C^+ and CO.

The ion-molecule reaction $C^+ + OH \rightarrow CO^+ + H$ with an estimated rate constant $k_2 \simeq 2 \times 10^{-9}$ cm^3 s^{-1} is assumed to be the limiting process in the series of reactions which culminates in CO formation through HCO^+. In view of the exothermicity of the $C^+ + OH$ process we consider its rate constant to be the same for $^{12}C^+$ and $^{13}C^+$.

The CO photodissociation rate is the product of the ultraviolet flux incident on a cloud and the self-shielding function where the latter function is dependent on position within a cloud. We write the rate as $\Gamma_i(s^{-1})$ where i denotes a particular isotopic species of CO ($i = 12$ for $^{12}C^{16}O$, $i = 13$ for $^{13}C^{16}O$). Values of Γ_{12} and Γ_{13} are estimated from van Dishoeck & Black (1988).

The isotopic exchange reaction is

$$^{13}C^+ + {}^{12}CO = {}^{13}CO + {}^{12}C^+ + \Delta E\,, \qquad (5)$$

where $\Delta E/k = 35$ K and we designate the rates as k_5^f for $^{13}C^+ + {}^{12}CO$ and k_5^r for the reverse reaction. Smith & Adams (1980) measured k_5^f at several temperatures; the result for the lowest temperature studied by them (80 K) is 6.8×10^{-10} cm^3 s^{-1}, and by the principle of detailed balance, $k_5^r = k_5^f \exp(-35/T)$. The rate constants k_5^f and k_5^r were measured with an accuracy of about 20%.

We assume that the three processes run to equilibrium. Then it is readily shown that the ratio of the ^{12}CO and ^{13}CO densities is given by

$$\frac{n(^{12}CO)}{n(^{13}CO)} \simeq \frac{n(^{12}C^+)}{n(^{13}C^+)} \frac{\Gamma_{13} + n(^{12}C^+)k_5^r}{\Gamma_{12} + n(^{12}C^+)k_5^f}\,. \qquad (6)$$

This expression was given earlier by Watson et al. (1976). If, as is likely, the C^+ ions are not fractionated, equation (6) gives

$$\frac{n(^{12}CO)}{n(^{13}CO)} = \left(\frac{^{12}C}{^{13}C}\right) \frac{\Gamma_{13} + n(^{12}C^+)k_5^f \exp(-35/T)}{\Gamma_{12} + n(^{12}C^+)k_5^f}\,. \qquad (7)$$

When photodissociation is much more important than isotopic exchange,

$$\frac{n(^{12}CO)}{n(^{13}CO)} = \frac{\Gamma_{13}}{\Gamma_{12}} \left(\frac{^{12}C}{^{13}C}\right),$$

and, since ^{12}CO will be more strongly self-shielded than ^{13}CO (i.e., $\Gamma_{12} < \Gamma_{13}$), $n(^{12}CO)/n(^{13}CO) > (^{12}C/^{13}C)$. If isotopic exchange is more important than photodissociation for both ^{12}CO and ^{13}CO,

$$\frac{n(^{12}CO)}{n(^{13}CO)} = \exp\left(-\frac{35}{T}\right)\left(\frac{^{12}C}{^{13}C}\right)$$

and $n(^{12}CO)/n(^{13}CO) < (^{12}C/^{13}C)$. There is an intermediate case that may be realized in the interior of a diffuse cloud where ^{13}CO may be lost primarily through photodissociation, but ^{12}CO may experience isotopic exchange in preference to photodissociation. Then, equation (7) gives

$$\frac{n(^{12}CO)}{n(^{13}CO)} = \frac{\Gamma_{13}}{n(^{12}C^+)k_5^f} \left(\frac{^{12}C}{^{13}C}\right).$$

Our spectroscopic measurements give the CO column densities [N(CO)] through the clouds. Along the line of sight, the degree of fractionation may vary, and, hence, it is necessary to integrate the expression for n(CO) to obtain N(CO) and a(CO). Here we suppose that $a(CO) \equiv N(^{12}CO)/N(^{13}CO) \cong n(^{12}CO)/n(^{13}CO)$ and evaluate a(CO) from equation (7) for the physical conditions of the clouds. We assume that carbon is essentially fully singly ionized. The total C abundance is taken to be the solar value ($A_C = 4 \times 10^{-4}$), and gaseous carbon is assumed to be depleted by a factor of 2: that is, $n(C^+) \simeq 2 \times 10^{-4} n_H$ where $n_H = n(H) + 2n(H) + 2n(H_2)$ is the total H density. Van Dishoeck & Black (1986a) consider $T = 60$ K and van Dishoeck et al. (1991) suggest $T = 40$ K to be appropriate for CO through the diffuse cloud; we adopt $T = 50$ K. With these assumptions equation (7) gives

$$a(CO) = 70 \frac{\Gamma_{13} + 6.8 \times 10^{-14} n_H}{\Gamma_{12} + 13.6 \times 10^{-14} n_H} = 150 \pm 27\,. \qquad (8)$$

Prediction of a(CO) from equation (8) calls for estimates of the rates Γ_i and the density n_H. Photodissociation rates Γ_{12} and Γ_{13} may be estimated from van Dishoeck & Black (1988, their eq. [3] and Table 5). If the cloud is illuminated on one side, $\Gamma_{12} \simeq 2 \times 10^{-12} I_{uv}[s^{-1}]$ and $\Gamma_{13}/\Gamma_{12} \simeq 3$ at a depth corresponding to $N(CO) \sim 2 \times 10^{15}$ cm^{-2}, $N(H_2) \sim 4 \times 10^{20}$ cm^{-2} and $A_v = 0.8$. The rates Γ_{12} and Γ_{13} increase toward the cloud's surface and Γ_{13}/Γ_{12} approaches unity: at the intermediate layer corresponding to $N(CO) \sim 1 \times 10^{15}$ cm^{-2}, $\Gamma_{12} \sim 1 \times 10^{-11} I_{uv}$ and $\Gamma_{13}/\Gamma_{12} \sim 2.2$. These estimates of Γ_{12} and Γ_{13} from van Dishoeck & Black (1988) are based on a model cloud that is not entirely appropriate for ζ Oph; for example, it was assumed that the CO was at an excitation temperature of $T_{ex} = 10$ K and quite turbulent ($b = 1.0$ km s^{-1} or $\Delta v = 1.7$ km s^{-1}), but the CO toward ζ Oph is less excited ($T_{ex} = 4$ K) and less turbulent ($\Delta v = 0.6$ km s^{-1}). On recalculation for the observed T_{ex} and Δv, the rates Γ_{12} and Γ_{13} will decrease, but the ratio Γ_{13}/Γ_{12} will increase. I_{uv} is formally a scale factor representing a local change of the ultraviolet radiation field over the general level proposed by Draine (1978). Here I_{uv} may also represent other uncertainties in the photodissociation rates due, for example, to incomplete or incorrect specification of the radiative transitions leading to photodissociation; then $I_{uv}(^{12}CO)$ is not necessarily equal to $I_{uv}(^{13}CO)$. The dependence of a(CO) on the density n_H is of special interest in view of the conflicting published estimates of n_H: for example, van Dishoeck et al. (1991) give $n_H \approx 250$ cm^{-3} for the layers containing diatomic molecules such as CO, but Viala, Roueff, & Abgrall (1988) offer high-density models with $n_H \sim 2500$ cm^{-3} as appropriate for ζ Oph. Absence of detectable CO $3 \rightarrow 2$ emission is used by van Dishoeck et al. to set an upper limit on the density, $n_H \lesssim 400$ cm^{-3}. The high-density models advocated by Viala et al. are in sharp conflict with the absence of CO $3 \rightarrow 2$ emission. The estimate $n_H \approx 250$ cm^{-3} is provided from an analysis of the populations of excited rotational levels of C_2 molecules (van Dishoeck & Black 1986b), while a similar density estimate of $n_H \approx 200$ cm^{-3} is derived from recent

© American Astronomical Society • Provided by the NASA Astrophysics Data System

1992ApJ...397..482S

results on collisional de-excitation of C_2 by H_2 (Lavendy et al. 1991).

At high densities the isotopic exchange reaction controls the fractionation and $a(CO) < 70$ is predicted unless I_{uv} is given quite unreasonably large values; for example, $n_H = 2500$ cm^{-3} in equation (8) gives $a(CO) = 45$ and 62 for $I_{uv} = 10$ in the core and the intermediate layer, respectively. On the other hand, equation (8) can be used to estimate n_H with the observed value of 150 ± 27 for $a(CO)$ and $I_{uv} \sim 10$. The core and intermediate cases then predict 77 (1 σ: 34–145) and 26 (1 σ: 0–260) cm^{-3}, respectively. The corresponding 3 σ ranges go from 0 to 600 and 1800 cm^{-3} for the two regimes, where the higher n_H values correspond to lower $a(CO)$ ratios. Use of kinetic temperatures lower than about 50 K, or of I_{uv} less than 10, would lead to lower estimates for n_H. Due to ζ Oph's propinquity, the ultraviolet radiation field incident upon the clouds is most probably more intense than the general field (i.e., $I_{uv} > 1$). When we take into account the uncertainties associated with the calculation of the photodissociation rates and the estimation of n_H from the C_2 level populations, we may consider that the observed fractionation is consistent with the prediction for a low-density model. The observed $a(CO)$ excludes high-density models with $I_{uv} \leq 10$.

Although high-density models may, in principle, explain the observed $a(CO)$ provided that I_{uv} is increased greatly (say, $I_{uv} \sim 200$–500 for $n_H = 2500$ cm^{-3}), this solution will exacerbate the well-known problem in accounting for the observed column density of CO: models with a much lower I_{uv} ($\simeq 4$) predict $N(CO)$ to be about an order of magnitude less than the observed value (van Dishoeck & Black 1986a). On the other hand, if I_{uv} is reduced to lessen the destruction of CO, the predicted $a(CO)$ will fall below the observed value and, in the limit, below the intrinsic value of 70. Resolution of the problem posed by the observed $N(CO)$ may lie in a combination of factors: for example, a faster rate of formation (k_2 is an estimate, not a result of a definitive measurement or calculation) and a modest reduction of the photodissociation rate, which is influenced by several factors (e.g., the strength of the photodissociating transitions, the shape and intensity of the incident spectrum below about 1000 Å). Van Dishoeck & Black's (1988) comprehensive discussion of Γ_{12} and Γ_{13} gives the impression that knowledge of the photodissociating transitions is such that Γ_{13}/Γ_{12} is probably calculable for diffuse clouds to within a factor of 2 or better. A small reduction of Γ_{12} is not ruled out, and, if Γ_{13} were increased by a similar factor, such a change could preserve the required fractionation of ^{13}CO relative to ^{12}CO, but it is unlikely that the observed and predicted $N(CO)$ can be reconciled and the observed fractionation of ^{13}CO relative to ^{12}CO reproduced solely by reducing the photodissociation of CO.

5.3. *The Excitation Temperature*

The ^{12}CO excitation temperature was estimated from the fit to the W_λ in Figure 3. As discussed earlier, the result, $T_{ex} = 4.2$ K, is dependent on the adopted values for the other parameters of the cloud model that affect the degree of saturation of the strong bands. We showed in Figure 4 that $T_{ex} = 4.2$ K provides a good fit to the rotational lines of $^{12}C^{16}O$ and the weak $^{13}C^{16}O$ lines of the A–X 5–0 band. Statistical equilibrium calculations of the lowest rotational levels of interstellar CO molecules have been reported by Smith et al. (1978) and van Dishoeck & Black (1987). Van Dishoeck & Black include optical depth effects in the radiative excitation of the rotational levels. Smith et al.'s calculations refer to clouds optically thin ($\tau_{CO} \to 0$) to CO lines. The results of the two studies are in good agreement for low CO column densities and show that the observed T_{ex} may be used to constrain the kinetic temperature and the H_2 density in the cloud: roughly, T_{ex} defines the product $n(H_2)T$.

As noted above, the temperature $T = 50$ K is appropriate for those layers contributing to the CO column density. The value $T_{ex} = 4.2$ K at $T = 50$ K is achieved at $n(H_2) \simeq 150$ cm^{-3} for $\tau_{CO} \to 0$. For $N(CO) \sim 2 \times 10^{15}$ cm^{-2}, a slightly lower limit on $n(H_2)$ is obtained. The estimates of $n(H_2)$ are based on the excitation temperature [$T_{ex}(1$–$0)$] defined by the populations of the rotational levels $J = 1$ and 0. The temperature $T_{ex}(2$–$1)$ is only a few tenths of a degree lower than $T_{ex}(1$–$0)$. This small difference is consistent with our assumption that $T_{ex}(1$–$0) = T_{ex}(2$–$1)$. For the core of the ζ Oph cloud, van Dishoeck & Black (1986a) suggest $T \simeq 25$ K, and at this temperature the observed T_{ex} corresponds to $n(H_2) \simeq 300$ cm^{-3} for $\tau_{CO} \to 0$ and $n(H_2) \simeq 150$ cm^{-3} for $N(CO) \sim 2 \times 10^{15}$ cm^{-2}. In the regions containing the CO molecules, much of the hydrogen is molecular: van Dishoeck et al. (1991) consider $n(H) \approx 0.5\ n(H_2)$ or $n_H \approx 1.5 n(H_2)$. Then, the observed and predicted T_{ex} are matched for $n_H \sim 200$ cm^{-3} at $T = 50$ K to $n_H \sim 300$ cm^{-3} at $T = 25$ K for $N(CO) \sim 2 \times 10^{15}$ cm^{-2}. Last, we used a large-velocity gradient code (LVG: Snell 1981, and references therein) to infer n_H from T_{ex}, treating each velocity component separately, and again found $n_H \sim 100$ cm^{-3}. The estimates do not change significantly for T between 40 and 60 K. Because the ^{13}CO rotational lines are optically thin, slightly higher densities are needed to produce $T_{ex} \sim 4$ K. Such estimates of n_H confirm the low values derived from analysis of the isotopic fractionation. Note that LVG ^{13}CO rotational temperatures differ by only a few tenths of a degree from T_{ex} of ^{12}CO, confirming their compatibility.

The warm gas responsible for the CH^+ line has a low density ($n_H \sim 100$ cm^{-3}). Hence the small amount of CO molecules in the warm gas is expected to have an excitation temperature close to that of the cosmic microwave background, say, $T_{ex} \sim 3$–4 K.

6. CONCLUDING REMARKS

Our analysis of the CO A–X bands has provided isotopic ratios $^{12}C^{16}O/^{13}C^{16}O = 150 \pm 27$ and $^{12}C^{16}O/^{12}C^{18}O > 800$ that constitute the strongest observational evidence for highly localized isotopic fractionation of CO in *diffuse* portions of an interstellar cloud ($A_v \sim 1$ mag). The value of the fractionation implies that selective photodissociation is the controlling influence of the fractionation. Unless the photodissociation rates of CO in the clouds have been very severely underestimated, the observed fractionation shows that the hydrogen density in the clouds is at the low end ($n_H \sim 100$–200 cm^{-3}) of the wide range previously suggested. This constraint on the density is consistent with the observed excitation temperature of CO.

Observational evidence for fractionation of ^{13}CO relative to ^{12}CO through the isotopic exchange reaction was presented earlier by Langer et al. (1989) and McCutcheon et al. (1980) from enhanced $^{13}C^{16}O$ radio emission relative to the emission of $^{12}C^{18}O$ in regions of dark clouds with $A_v \leq 4$ mag. The analyses, however, are based on the assumption that the $^{12}C^{16}O$-to-$^{12}C^{18}O$ ratio is constant. The results are probably better described as fractionation of $^{13}C^{16}O$ relative to $^{12}C^{18}O$

© American Astronomical Society • Provided by the NASA Astrophysics Data System

1992ApJ...397..482S

through selective isotopic photodissociation much like what we find for $^{12}CO/^{13}CO$ in the gas toward ζ Oph. The isotopic exchange reaction is not important in this case because the temperatures in these regions are usually comparable to or greater than the zero-point energy differences.

The $^{12}C/^{13}C$ ratio of carbon monoxide in the *cores* of nearby molecular clouds is typically 60 (Wannier 1980; Langer & Penzias 1990). The observations of Langer & Penzias are particularly noteworthy because their result is based on data for two rare isotopic species, $^{12}C^{18}O$ and $^{13}C^{18}O$, in cloud cores where photodissociation of CO is unimportant and carbon is predominantly neutral. Indeed, under these conditions CO is not expected to be fractionated. The $^{12}C/^{13}C$ ratio for cloud cores compares favorably with recent results for CH^+. The difference from the solar system ratio of 90 indicates that nucleosynthetic processing has occurred since the solar system formed.

We thank C. M. Brown for providing accurate measurements of the wavelengths of CO lines, F. Rostas for experimental data on oscillator strengths in advance of publication, and N. J. Evans II for the LVG code. We thank the referee, W. D. Langer, for his suggested revisions. D. L. L. and Y. S. were supported in part by NASA contract NAG5-1616. S. R. F. was supported by the NASA RTOPs program and funded through the Jet Propulsion Laboratory. J. A. C. acknowledges support for his involvement with the GHRS through NASA contract NAS5-29638 and grant NAGW-2520.

REFERENCES

Anicich, V. G., & Huntress, W. J. 1986, ApJS, 62, 553
Bally, J., & Langer, W. D. 1982, ApJ, 255, 145; erratum 261, 747
Cardelli, J. A., Ebbets, D. C., & Savage, B. D. 1990, ApJ, 365, 789
———. 1992, in preparation
Cardelli, J. A., Savage, B. D., Bruhweiler, F. C., Smith, A. M., Ebbets, D. C., Sembach, K., Jr., & Sofia, U. J. 1991, ApJ, 377, L57
Cardelli, J. A., Savage, B. D., & Ebbets, D. C. 1991, ApJ, 383, L23
Crane, P., Hegyi, D. J., & Lambert, D. L. 1991, ApJ, 378, 181
Crutcher, R. M., & Federman, S. R. 1987, ApJ, 316, L71
Crutcher, R. M., & Watson, W. D. 1981, ApJ, 244, 855
Draine, B. T. 1978, ApJS, 36, 595
———. 1986, ApJ, 310, 408
Duncan, D. K., & Ebbets, D. C. 1989, Goddard High Resolution Spectrograph Instrument Handbook (Baltimore: Space Telescope Science Institute)
Eidelsberg, M., Roncin, J.-Y., Le Floch, A., Launay, F., Letzelter, C., & Rostas, J. 1987, J. Molec. Spectrosc., 121, 309
Eidelsberg, M., Rostas, F., Breton, J., & Thieblemont, B. 1992, J. Chem. Phys., in press
Elitzur, M., & Watson, W. D. 1980, ApJ, 236, 172
Federman, S. R. 1982, ApJ, 257, 125
———. 1986, ApJ, 309, 306
Field, R. W., Benoist D'Azy, O., Lavollée, M., Lopez-Delgado, R., & Tramer, A. 1983, J. Chem. Phys., 78, 2838
Glassgold, A. E., & Langer, W. D. 1976, ApJ, 206, 85
Hawkins, I., & Jura, M. 1987, ApJ, 317, 926
Hawkins, I., Jura, M., Meyer, D. M., & Craig, L. 1989, BAAS, 21, 1142
Hobbs, L. M. 1973, ApJ, 180, L79
Jenkins, E. B., Drake, J. F., Morton, D. C., Rogerson, J. B., Spitzer, L., & York, D. G. 1973, ApJ, 181, L122
Kirby, K., & Cooper, D. L. 1989, J. Chem. Phys., 90, 4895
Krishnakumar, E., & Srivastava, S. K. 1986, ApJ, 307, 795
Kurucz, R. L. 1976, Smithsonian Astrophys. Obs., Spec. Rept. 374
Lambert, D. L., Sheffer, Y., & Crane, P. 1990, ApJ, 359, L19
Langer, W. D., Glassgold, A. E., & Wilson, R. W. 1987, ApJ, 322, 450 (LGW)
Langer, W. D., Goldsmith, P. F., Carlson, E. R., & Wilson, R. W. 1980, ApJ, 235, L39
Langer, W. D., & Penzias, A. A. 1990, ApJ, 357, 477
Lassettre, E. N., & Skerbele, A. 1971, J. Chem. Phys., 54, 1597
Lavendy, H., Robbe, S. M., Chambaud, G., Levy, B., & Roueff, E. 1991, A&A, 251, 365
Le Bourlot, J., Gerin, M., & Perault, M. 1989, A&A, 219, 179
Le Floch, A., Rostas, J., & Rostas, F. 1990, Chem. Phys., 142, 261
Mantz, A. W., Maillard, J.-P., Roh, W. B., & Rao, K. N. 1975, J. Molec. Spectrosc., 57, 155
McCutcheon, W. H., Dickman, R. L., Shuter, W. L. H., & Roger, R. S. 1980, ApJ, 237, 9
Messing, I., Filseth, S. V., Sadowski, C. M., & Carrington, T. M. 1981, J. Chem. Phys., 74, 3874
Mitchell, G. F., & Watt, G. D. 1985, A&A, 151, 121
Morton, D. C. 1975, ApJ, 197, 85
Savage, B. D., Cardelli, J. A., & Sofia, U. J. 1992, ApJ, submitted
Smith, A. M., Krishna Swamy, K. S., & Stecher, T. P. 1978, ApJ, 220, 138
Smith, D., & Adams, N. G. 1980, ApJ, 242, 424
Snell, R. L. 1981, ApJS, 45, 121
Stahl, O., & Wilson, T. L. 1992, A&A, 254, 327
Stahl, O., Wilson, T. L., Henkel, C., & Appenzeller, I. 1989, A&A, 221, 321
Tilford, S. G., & Simmons, J. D. 1972, J. Phys. Chem. Ref. Data, 1, 147
van Dishoeck, E. F., & Black, J. H. 1986a, ApJS, 62, 109
———. 1986b, ApJ, 307, 332
———. 1987, in Physical Processes in Interstellar Clouds, ed. G. E. Morfill & M. Scholer (Dordrecht: Reidel), 241
———. 1988, ApJ, 334, 771
van Dishoeck, E. F., Black, J. H., Phillips, T. G., & Gredel, R. 1991, ApJ, 366, 141
Viala, Y. P., Roueff, E., & Abgrall, H. 1988, A&A, 190, 215
Wannier, P. G. 1980, ARA&A, 18, 399
Wannier, P. G., Penzias, A. A., & Jenkins, E. B. 1982, ApJ, 254, 100 (WPJ)
Watson, W. D., Anicich, V. G., & Huntress, W. J. 1976, ApJ, 205, L165

© American Astronomical Society • Provided by the NASA Astrophysics Data System